

Total-Ionizing-Dose Effects at Ultra-High Doses in AlGa_N/Ga_N HEMTs

Stefano Bonaldo, *Member, IEEE*, En Xia Zhang, *Senior Member, IEEE*, Serena Mattiazzo, Alessandro Paccagnella, *Senior Member, IEEE*, Simone Gerardin, *Member, IEEE*, Ronald D. Schrimpf, *Fellow, IEEE*, and Daniel M. Fleetwood, *Fellow, IEEE*,

Abstract— Total-ionizing-dose effects in AlGa_N/Ga_N HEMTs are evaluated by DC and low frequency noise measurements. Devices with and without passivation layers are irradiated with 10-keV X-rays up to 100 Mrad(SiO₂) under different bias conditions. Irradiated devices show significant electrical shifts in threshold voltage and transconductance. At doses <10 Mrad(SiO₂), the TID-induced effects are related to the passivation of pre-existing acceptor-like defects via hole capture, which induces negative threshold voltage shifts and improvement of transconductance. At doses >10 Mrad(SiO₂), dehydrogenation of defects and impurity complexes leads to the creation of acceptor-like defects, which degrade the transconductance, shift positively the threshold voltage, and increase the low-frequency noise. Effects are enhanced in unpassivated devices and when the gate is biased at high voltage.

Index Terms—Total ionizing dose, AlGa_N HEMTs, DC, low frequency noise, charge trapping, bias condition.

I. INTRODUCTION

THE demands on electronics working in harsh radiation environments have increased in the last several decades. Experimental fusion reactor facilities, nuclear waste depositories, and next-generation particle accelerators require chips able to withstand ultra-high ionizing radiation doses on the order of >10 Mrad(SiO₂). For example, the trackers of the future High-Luminosity Large Hadron Collider (HL-LHC) at CERN, Switzerland, will be exposed to total ionizing doses (TIDs) up to 1 Grad(SiO₂) over ten years of operation [1].

TID effects at ultra-high doses above ~10 Mrad(SiO₂) have been investigated in Si-based planar and FinFET technologies [2]-[12]. Studies at 1 Grad(SiO₂) on 65 nm MOSFETs [2]-[4], 31 nm MOSFETs [6]-[8], 16 nm FinFETs [9]-[11], and Gate-All-Around FETs [12] have revealed issues related to radiation-induced charge buildup in dielectrics, e.g., in shallow trench isolation (STI) and in spacers and have underlined the important role of hydrogen transport for the activation of TID-induced traps.

On the other hand, power and RF systems often incorporate compound semiconductor devices, including Ga_N-based high-electron mobility transistors (HEMTs). AlGa_N/Ga_N HEMTs are widely used in high-power and radio-frequency applications

due to their enhanced carrier mobility in the two-dimensional electron gas (2DEG) and their high breakdown electric field [13]. The absence of gate dielectrics in AlGa_N/Ga_N devices is a key factor for their high tolerance to ionizing radiation [14]. However, in the last ~10 years, several works have pointed out significant TID sensitivities of AlGa_N/Ga_N HEMTs; these may prevent the proper functioning at the relatively low doses typical of space applications and are likely to be even larger in high-radiation applications [15]-[23].

X-ray and 1.8-MeV proton irradiations revealed that AlGa_N/Ga_N HEMTs often exhibit threshold voltage shifts and reductions in transconductance [15]-[17]. These TID and DD effects are related primarily to trap activation and/or neutralization in the AlGa_N and Ga_N layers with strong sensitivities to the bias applied during irradiation [15],[16]. Results of proton irradiations are often complicated to interpret, as they combine TID effects with displacement damage (DD) effects. X-ray irradiations in recent works focused on the exploration of pure TID mechanisms in AlGa_N/Ga_N HEMTs. However, the cumulative dose in these studies is typically <1 Mrad(SiO₂), much lower than the TID often induced by proton irradiations, which is often >10 Mrad(SiO₂) [15], [16], [18]. Hence, the pure TID response of Ga_N HEMTs at ultra-high doses is still unknown. Its exploration is useful for improving knowledge of basic degradation mechanisms in Ga_N-based HEMTs.

This work explores ultra-high-dose effects in a development-stage AlGa_N/Ga_N HEMT technology through DC and low frequency noise measurements. The results evidence complex synergies between TID effects and electrical stress, each of which is strongly influenced by applied biases. The largest threshold-voltage shifts are observed for this technology when negative gate bias is applied during irradiation, i.e., when devices are irradiated in the OFF state. In contrast, the largest

TABLE I
BIAS CONDITIONS DURING IRRADIATION AND ANNEALING.*

Bias condition	V_g [V]	V_d [V]	V_s [V]
<i>GND</i>	0	0	0
<i>ON</i>	0	+10	0
<i>CUT-OFF</i>	-7	+10	0
<i>OFF</i>	-7	0	0

*The substrate is always biased at 0 V. The annealing bias condition is identical to the bias condition applied during the irradiation.

S. Mattiazzo is with the Department of Physics and Astronomy, University of Padova and INFN Sezione di Padova, 38134 Padova, Italy.

E. X. Zhang, R. D. Schrimpf, and D. M. Fleetwood are with the Department of Electrical and Computer Engineering, Vanderbilt University, Nashville, TN 37235, USA.

Manuscript submitted October 31, 2022.

The portion of the work performed at Vanderbilt University was supported in part by the US Air Force Center of Excellence in Radiation Effects, Award FA9550-22-1-0012.

S. Bonaldo, A. Paccagnella and S. Gerardin are with the Department of Information Engineering, University of Padova, 38134 Padova, Italy (email: stefano.bonaldo@unipd.it).

transconductance degradation occurs under ON bias irradiation. Unpassivated devices show larger sensitivity to TID irradiation and bias stress than passivated devices, reinforcing the strong role of hydrogen transport and reactions on the radiation response and reliability of GaN-based HEMTs.

II. DEVICES AND EXPERIMENTAL DETAILS

A. Devices under test

The GaN HEMTs under test were fabricated in a development-stage AlGaIn/GaN technology at the University of California, Santa Barbara (UCSB), USA [22]. The active region consists of 200 nm of unintentionally doped (UID) GaN that is grown by Ga-rich plasma-assisted molecular beam epitaxy on n-type free-standing GaN substrate having layer doped with Fe and C (Fig. 1). The transistor channel width is 150 μm and the channel length L_g is 0.7 μm , with gate-to-drain separation (L_{gd}) of 1 μm and gate-to-source separation (L_{gs}) of 0.5 μm . Transistors in this study are built in two configurations: (1) passivated by a thick SiN_x layer (normal configuration) and (2) unpassivated (for comparison), as shown in Figs. 1(a) and (b).

B. Test conditions

Irradiation tests were conducted using a 10-keV X-ray irradiator at a dose rate of 3.8 Mrad(SiO₂)/h for a total exposure

time of ~ 29 h to reach 100 Mrad(SiO₂). All doses and rates are referred to equilibrium doses in SiO₂ for consistency in calibration and to facilitate comparison with other works [15]-[19]. Considering the relative atomic numbers, we infer from comparative studies of similar materials that the doses in GaN may be 2x-2.5x the quoted equilibrium SiO₂ dose [24]-[26].

The radiation exposure was stopped at several steps. At each step, devices were kept with all terminals grounded for about 60 s before transistors were electrically characterized. This minimizes annealing time and allows the device to stabilize before measurements. After completion, devices were annealed at room temperature (RT) for 27 h. Several bias configurations were applied to the HEMTs during irradiation and annealing, as shown in Table I. The DC static response and low-frequency noise of the transistors were measured at room temperature before exposure and at several irradiation steps. At least two devices were tested for each set of conditions; representative results are shown below. The threshold voltage V_{th} is defined as $V_{gs-int} - V_{ds}/2$; V_{gs-int} is extracted in the linear region ($V_{ds} = 0.1$ V) as the gate-voltage axis intercept of the linear extrapolation of the I_d - V_{gs} curve at the point of its maximum first derivative.

C. Evaluation of electrical stress effects

Irradiations up to 100 Mrad(SiO₂) require about ~ 29 h. To distinguish degradation induced by electrical stress from that induced by irradiation, the GaN-based HEMTs were stressed

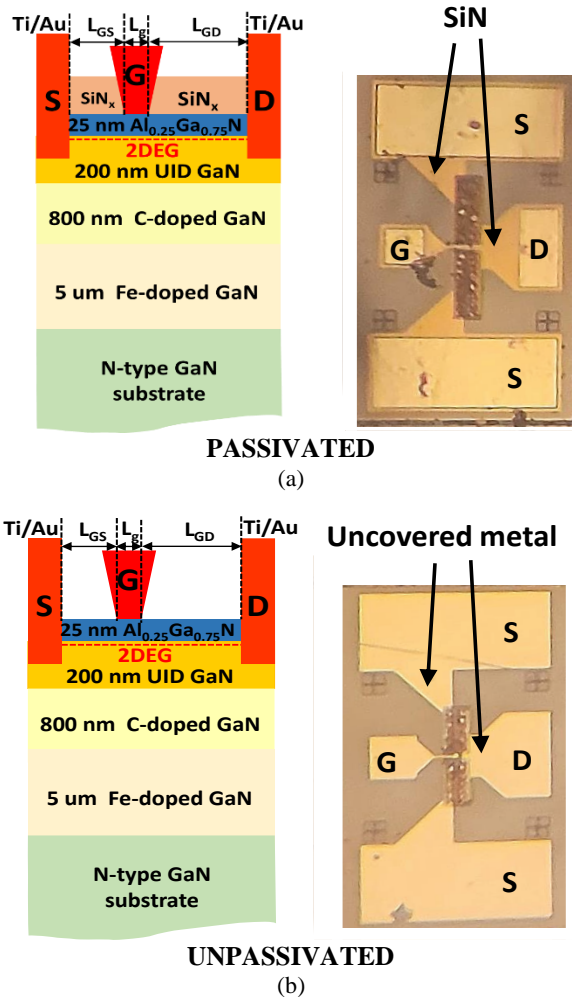


Fig. 1. Schematic diagram of stack layers of AlGaIn/GaN HEMTs (not to scale) and optical microscope images of (a) passivated and (b) unpassivated GaN-based HEMTs.

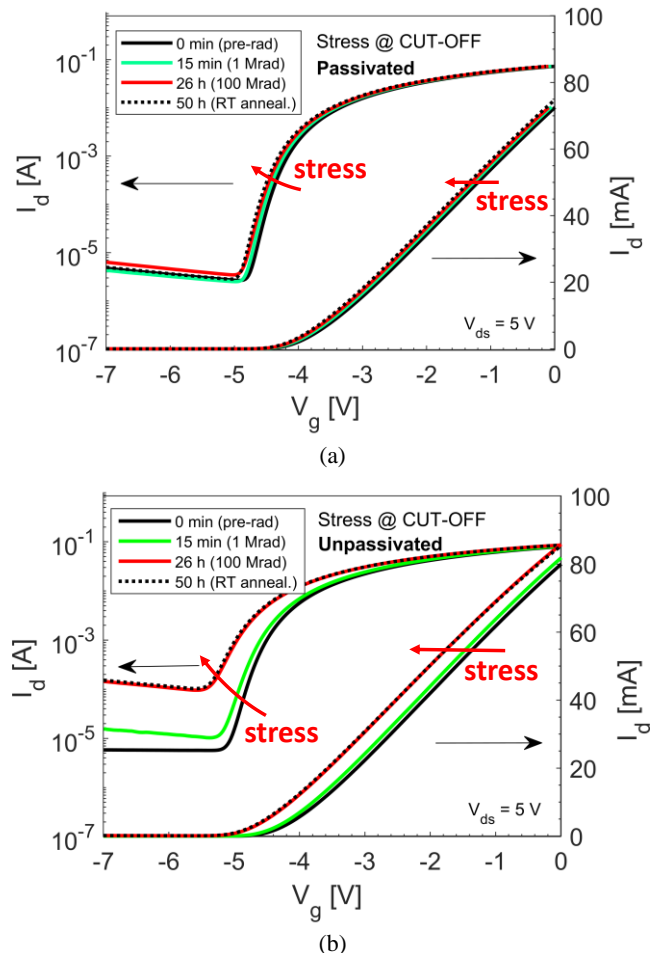


Fig. 2. Electrical stress-induced degradation of I_d - V_{gs} curves in the saturation regime ($V_{ds} = 5$ V) for (a) passivated and (b) unpassivated AlGaIn HEMTs. The devices were biased for a total time of 50 h at room temperature in the cut-off bias, in order to evaluate the degradation induced by the electrical stress without X-ray exposure.

without X-ray under the bias conditions of Table I for the same amounts of time required for devices to be irradiated up to 100 Mrad(SiO₂).

Fig. 2 shows the electrical stress-induced degradation for (a) passivated and (b) unpassivated devices irradiated in “CUT-OFF”-bias condition, which is the case in which the largest parametric shifts are observed. The stressed HEMTs exhibit increases in leakage current and shifts of threshold voltage V_{th} . The V_{th} undergoes a negative and rapid shift in the first 1 hour. After ~29 h, the passivated HEMT biased in the “CUT-OFF” condition shows an increase of maximum drain current of 4%, while the passivated HEMT shows a decrease of maximum on-current of 7%. For all biases, the unpassivated HEMTs show greater degradation than passivated devices.

Often electrical-stress induced effects of HEMTs may be substantial and comparable to the TID-induced effects. For this reason, the next sections report and compare the responses of biased irradiated and unirradiated devices at similar times.

III. PASSIVATED DEVICES

A. TID tolerance at different bias conditions

The DC characteristics in the saturation regime ($V_{ds} = 5$ V) of passivated GaN-based HEMTs are shown in Fig. 3 when

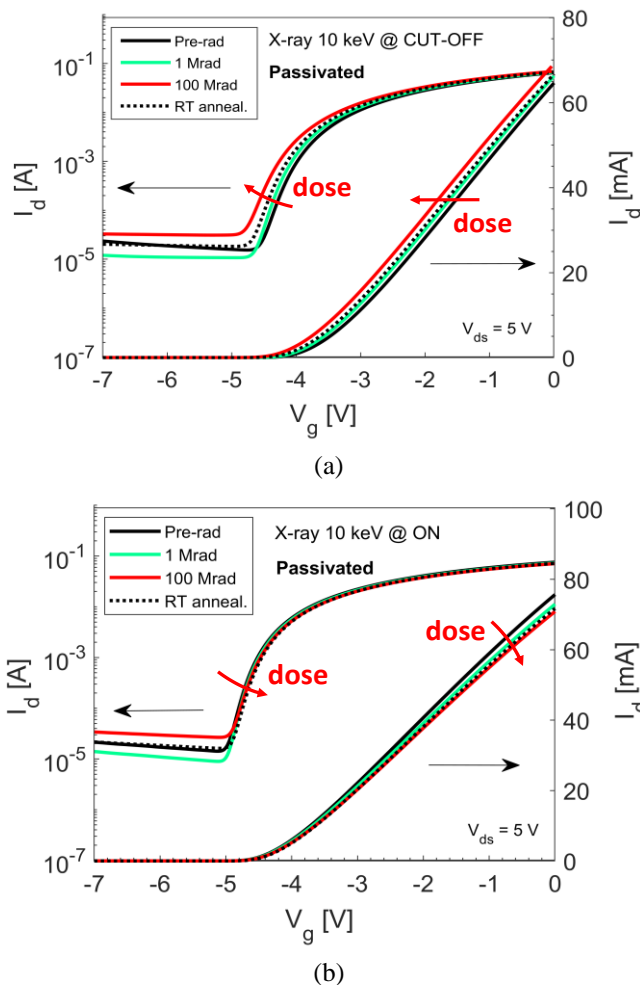


Fig. 3. I_d - V_{gs} curves of passivated GaN-based HEMTs in the saturation regime ($V_{ds} = 5$ V). The devices were irradiated up to 100 Mrad(SiO₂) and then annealed at room temperature for 27 h in (a) the “CUT-OFF”-bias and (b) the “ON”-bias.

devices are irradiated and annealed under the “CUT-OFF” and “ON”-bias conditions. During exposure, the drain leakage current at $V_g=0$ V increases significantly regardless of the applied bias, a signature of drain-to-gate leakage. The V_{th} shifts monotonically to negative values as large as -270 mV in “CUT-OFF”-biased devices, and to positive values up to 50 mV in “ON”-biased devices. The “ON”-biased devices exhibit degradation of the transconductance g_m , which is evident as decreases in the slopes of the I_d - V_g curves for -3 V $< V_g < 0$ V. Slight performance recovery is visible after 27 h of room temperature annealing, suggesting the formation of a significant density of stable defects.

Fig. 4 shows the effects of applied bias on the degradation of the maximum drain current I_{on} , defined here as the drain current at $V_{gs} = 0$ V and $V_{ds} = 5$ V. Dotted lines refer to electrical stress-induced degradation without X-ray exposure; continuous lines are obtained with X-ray exposure. GaN HEMTs irradiated in the “CUT-OFF” and “OFF” biases show increases (improvement) in I_{on} by about 9% and 7% at 100 Mrad(SiO₂). Room temperature annealing reduces this increase: $\Delta I_{on} = 4\%$ after 27 h. The significant difference between the continuous and dotted lines demonstrates that the performance enhancement of “CUT-OFF” and “OFF” biased devices is affected more strongly by TID-induced effects than by bias-induced effects. In contrast, devices irradiated in the “ON” bias condition exhibit a degradation, as evidenced by the 5% decrease of I_{on} at 100 Mrad(SiO₂). The degradation for devices irradiated or electrically stressed in the “ON”-bias condition is similar, showing that bias-induced stress dominates the changes in device response.

Fig. 5 shows the radiation-induced degradation of the DC parameters (a) ΔV_{th} and (b) maximum transconductance Δg_{m-MAX} , calculated in the linear regime at $V_{ds} = 0.5$ V. These values are for different GaN-based HEMTs irradiated and then annealed under different bias conditions. The I_{on} variation of irradiated GaN HEMTs of Fig. 4 is dominated by the negative shift of V_{th} for “CUT-OFF” and “OFF”-biased devices. Three interesting effects are evident in Fig. 5:

1) *Insensitivity to TID when irradiated at 0 V gate bias.* The best TID tolerance is found for “GND”-biased and “ON”-

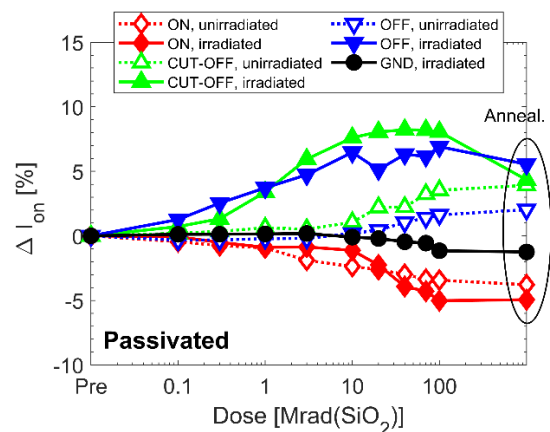


Fig. 4. Degradation of maximum drain current ΔI_{on} as a function of dose in passivated GaN-based HEMTs. Dotted lines refer to the electrical stress-induced degradation, where devices were tested without X-ray exposure; continuous lines refer to test results with X-ray exposure. Irradiations were performed up to 100 Mrad(SiO₂) and then devices were annealed at room temperature for 27 hours in different bias conditions.

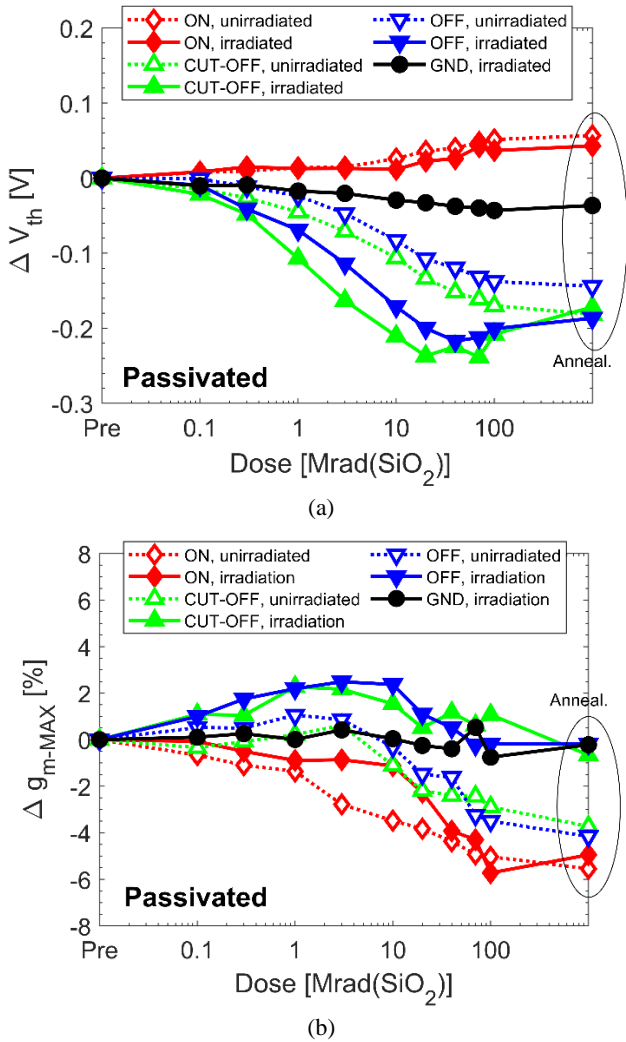


Fig. 5. Degradation of (a) threshold voltage ΔV_{th} and (b) maximum transconductance Δg_{m-MAX} as a function of dose in passivated GaN-based HEMTs. Dotted lines refer to electrical stress-induced degradation without X-ray exposure; continuous lines refer to test results with X-ray exposure. Irradiations were performed up to 100 Mrad(SiO₂); then devices were annealed at room temperature for 27 h in different bias conditions.

biased devices, for which the gate bias is 0 V. This enhancement of the TID tolerance is most likely related to the limited charge yield at low electric fields [15],[16],[27]. The “ON”-biased devices show a slight V_{th} increase and g_m decrease, but this degradation is related to a bias-stress-induced effect, as shown by the overlapping of the continuous and dotted (red) curves. It is more likely that “ON”-biased devices suffer from hot-electron stress, which can induce the activation of acceptor-like traps through the dehydrogenation of O_N-H complexes in the GaN buffer layer [15],[17],[19]. In the case of “ON”-biased devices, post-irradiation annealing continues to induce a slight increase of the V_{th} , as “ON” bias is maintained for longer times.

2) *Rebound of the V_{th} shifts at 10 Mrad(SiO₂) of irradiated HEMTs.* Irradiations in the “CUT-OFF” and “OFF” conditions induce an initial negative V_{th} shift. At 10 Mrad(SiO₂), the ΔV_{th} is about -280 mV for the “CUT-OFF”-biased HEMTs and -263 mV for “OFF”-biased HEMTs. The negative V_{th} shift and the increase of g_{m-MAX} indicates neutralization of acceptor-like defects [28]. After 10 Mrad(SiO₂), V_{th} recovers somewhat, as

shown by the positive trend vs. dose. At 100 Mrad(SiO₂), ΔV_{th} is about -190 mV for both “CUT-OFF” and “OFF”-biased HEMTs and it continues to recover during the RT annealing.

3) *Rebound of g_{m-MAX} at 10 Mrad(SiO₂) of irradiated HEMTs.* At doses <10 Mrad(SiO₂), the g_{m-MAX} of irradiated HEMTs increases with cumulative dose at a higher rate compared to electrically stressed devices, consistent with accelerated acceptor neutralization [17]. At doses >10 Mrad(SiO₂), g_{m-MAX} degrades, suggesting activation of defects in the active GaN layer [15], [17], [19]. Increases of acceptor-like defect densities in the 2DEG may lead to TID-induced transconductance loss and positive V_{th} shifts, i.e., formation of N vacancies, Ga vacancies, and/or O_N DX centers [15], [16], [18], [20], [29].

B. Low frequency noise responses

Additional insight into densities of defects contributing to charge trapping are obtained by low-frequency noise measurements [15], [16], [18], [30]-[33]. The drain-voltage noise power spectral density S_{pd} was evaluated in a frequency span between 1 Hz and 1 kHz at $|V_{ds}| = 0.1$ V for several values of $V_{gt} = V_{gs} - V_{th}$. The low-frequency noise of GaN-based HEMTs is caused primarily by fluctuations of the numbers of carriers induced by the capture and emission of carriers at individual defect sites in the GaN layer or at the AlGaN/GaN border, which is often affected by the atomic reconfiguration of single defect sites in the GaN [27],[29].

Fig. 6 shows the low-frequency noise for (a) “CUT-OFF”-biased and “ON”-biased HEMTs before irradiation, at 1 Mrad(SiO₂), at 100 Mrad(SiO₂), and after high temperature annealing. GaN-based HEMTs show typical 1/f low-frequency noise. In “ON”-biased HEMTs, the noise is constant and is relatively insensitive to the irradiation and electrical stress. On the other hand, the noise magnitude of “CUT-OFF”-biased devices is approximately constant at 1 Mrad(SiO₂) and increases at 100 Mrad(SiO₂). This increase of the noise, which is visible only at ultrahigh doses, indicates activation of new traps, in agreement with the V_{th} increases and g_m decreases occurring at > 10 Mrad(SiO₂) in Fig. 5. During room temperature annealing, very little change occurs to the noise.

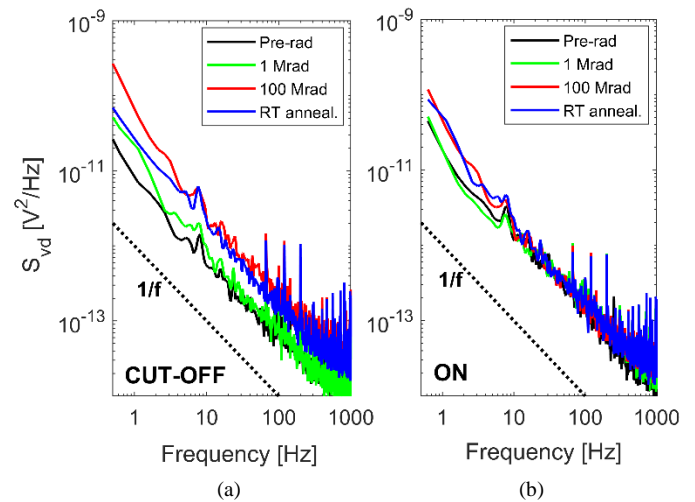


Fig. 6. Low-frequency noise magnitudes for GaN-based HEMTs irradiated and annealed in (a) the “CUT-OFF”-bias condition and (b) “ON”-bias condition. The noise was measured at $V_{ds} = 0.5$ V and $V_{gt} = 0.6$ V at room temperature.

To investigate the density distributions in space and energy of the border traps, Fig. 7 plots the low-frequency noise magnitude at 10 Hz as a function of $V_{gt} = V_{gs} - V_{th}$ in GaN-based HEMTs irradiated in “CUT-OFF” and “ON”-bias conditions. When the slope $|\beta|$ of the $S_{vD}-V_{gt}$ curve is approximately equal to 2, the effective density of the border traps is uniform in space and energy [27]-[29], [33], [34]. “CUT-OFF”-biased devices show a significant increase of low-frequency noise levels at 100 Mrad(SiO₂) in agreement with Fig. 6(a). In both pristine and irradiated devices, the slope $|\beta|$ of $S_{vD}-V_{gt}$ is ~ 2.1 , indicating an approximately uniform spatial and energetic distribution of traps [27]-[29]. The slope $|\beta|$ of $S_{vD}-V_{gt}$ is ~ 2.5 after the RT annealing, suggesting a less uniform density of generated traps in space and energy. On the other hand, “ON”-biased devices are characterized by constant noise with $|\beta|$ equal to 2, indicating uniform and constant density of traps. Room temperature annealing in “ON”-biased devices induces a slight increase in $|\beta|$, which is equal to 2.3 after 27 h of room temperature annealing.

IV. UNPASSIVATED DEVICES

A. TID sensitivity

This section analyzes the TID response of unpassivated devices that are otherwise similar to those in Figs. 3-7. The DC characteristics in the linear regime ($V_{ds} = 0.1$ V) of unpassivated

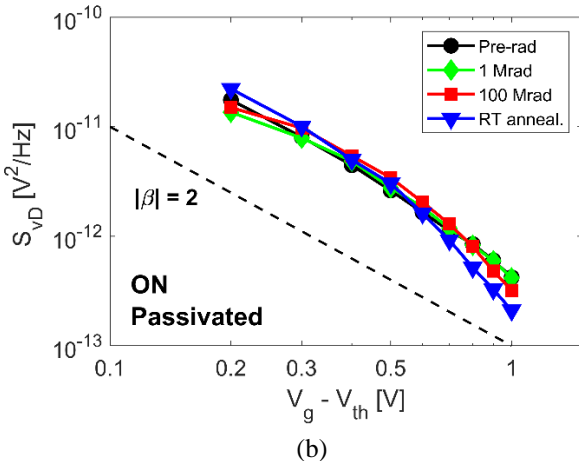
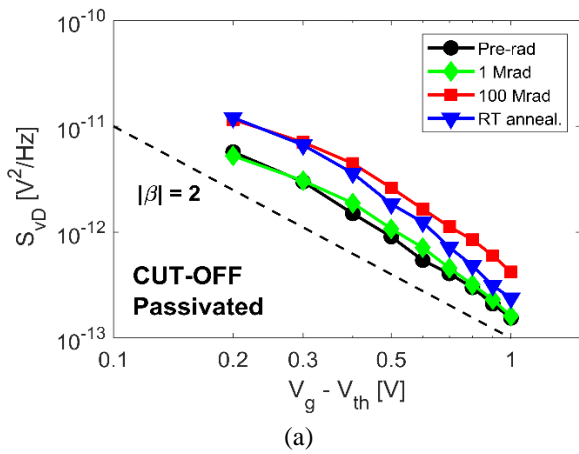


Fig. 7. $1/f$ noise magnitudes at $f = 10$ Hz vs. $V_{gs}-V_{th}$ at $V_{ds} = 0.5$ V for GaN-based HEMTs with irradiated and annealed in (a) the “CUT-OFF”-bias condition and (b) “ON”-bias condition.

GaN-based HEMTs are shown in Fig. 8 when the devices are irradiated and annealed in the “CUT-OFF” and “ON”-bias conditions. The highest shift is visible in the “CUT-OFF” condition, where V_{th} shifts to negative values by about ~ 0.6 V and the leakage current increases by two orders of magnitude, from 2×10^{-6} A to 2×10^{-4} A. Slight performance recovery is visible after 27 h of room temperature annealing, similarly to passivated devices. The “ON”-biased devices are characterized by negative V_{th} shifts, about -270 mV after 100 Mrad(SiO₂), which are smaller than those of “CUT-OFF”-biased devices.

The influence of irradiation bias on TID sensitivity is shown in Fig. 9, which summarizes the degradation of: (a) maximum drain current I_{on} , (b) threshold voltage V_{th} , and (c) maximum transconductance g_{m-MAX} . The dotted lines refer to electrical stress-induced degradation without X-ray exposure; continuous lines are obtained with X-ray exposure. The I_{on} variation of irradiated GaN HEMTs of Fig. 9(a) is mostly dominated by the negative shift of V_{th} . The highest shift is visible in “CUT-OFF” and “OFF” biases, while the bias conditions with the smallest degradation are the “GND” and “ON” conditions. The clear separation of dotted and continuous lines indicates that the degradation induced during the exposure is mainly related to TID.

In contrast to the passivated HEMTs, the V_{th} values of unpassivated devices irradiated in “GND” and “ON” conditions

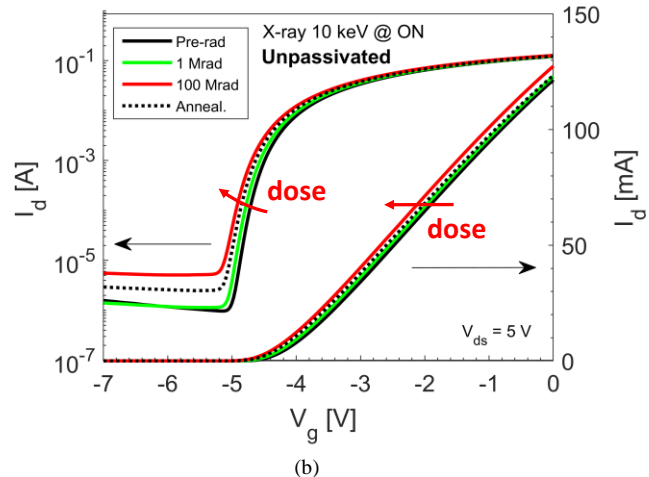
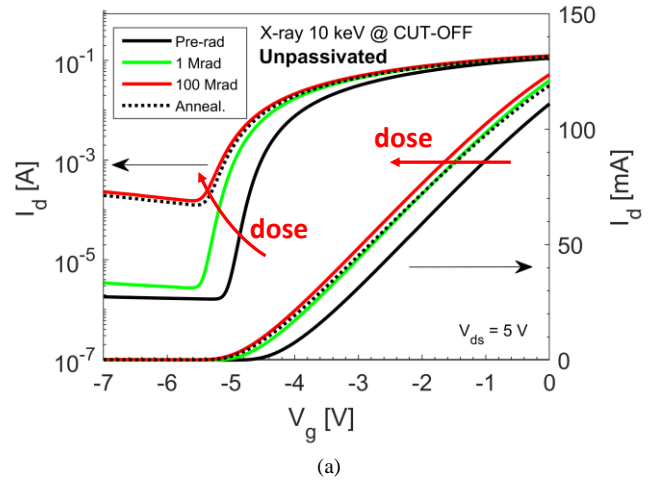


Fig. 8. I_d-V_{gs} curves of unpassivated GaN-based HEMTs in the saturation regime ($V_{ds} = 5$ V). The devices were irradiated up to 100 Mrad(SiO₂) and then annealed at room temperature for 27 h in (a) the “CUT-OFF”-bias and (b) the “ON”-bias.

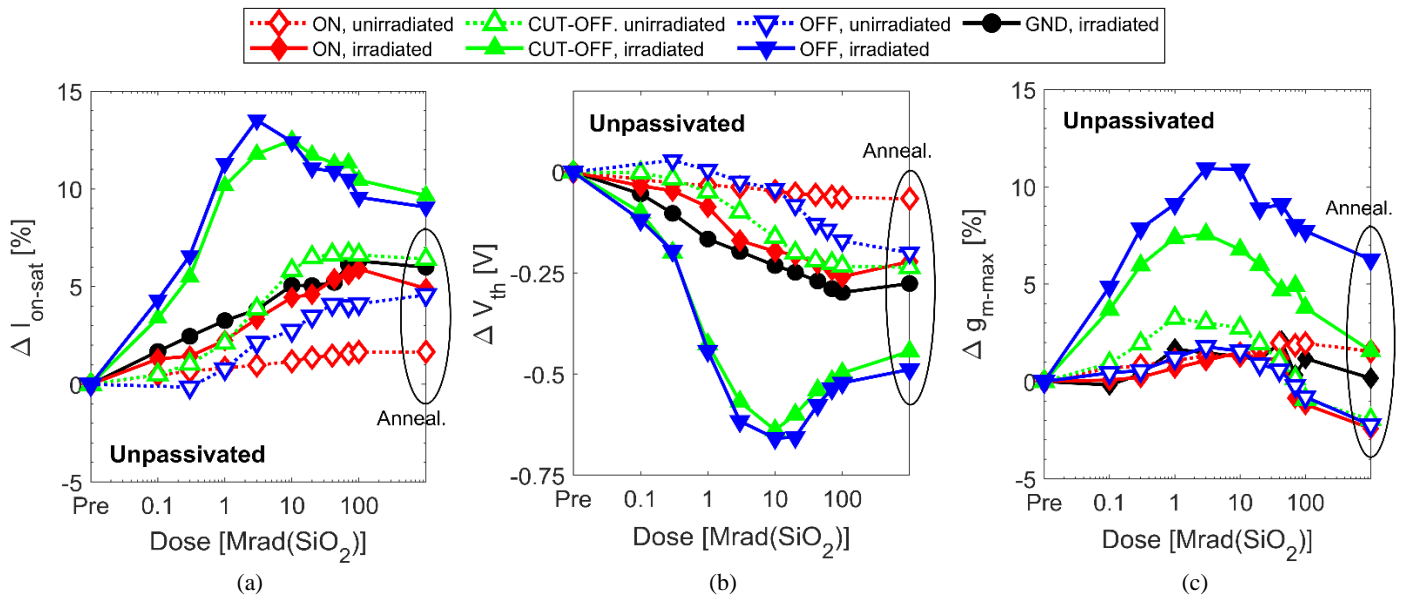


Fig. 9. Degradation of (a) maximum drain current ΔI_{on-sat} , (b) threshold voltage ΔV_{th} , and (c) maximum transconductance Δg_{m-MAX} as a function of dose in unpassivated GaN-based HEMTs. Dotted lines refer to electrical stress-induced degradation, where devices were tested without X-ray exposure; continuous lines refer to test results with X-ray exposure. Irradiations are performed up to 100 Mrad(SiO₂) and then devices were annealed at room temperature for 27 h in different bias conditions.

degrade with a similarly decreasing monotonic trend. On the other hand, similarly to passivated devices, the “CUT-OFF” and “OFF”-biased transistors exhibit a rebound of the V_{th} and g_m values around 10 Mrad(SiO₂). At doses < 10 Mrad(SiO₂), V_{th} shifts to negative values and g_m increases. At doses > 10 Mrad(SiO₂), V_{th} shifts toward more positive values and g_m decreases.

Fig. 10 shows ΔV_{th} as a function of the time for devices that were irradiated in the OFF-bias condition and then annealed at room temperature for up to 24 h in the same bias condition. In the passivated devices, V_{th} recovers by 34 mV in the first 5 h and by 40 mV after 24 h. In unpassivated devices, V_{th} recovers by 79 mV in the first 5 h and by 103 mV after 24 h. The plot shows that most annealing-induced shifts occur in the first 5 h with the highest shifts in unpassivated devices. The recovery then saturates, becoming approximately stable for annealing times over 15 h. The additional annealing that occurs in the unpassivated devices is most likely due to enhanced hydrogen

diffusion and passivation reactions in these devices [21], [23], as discussed in Section V.

Low-frequency noise measurements for the “CUT-OFF”-biased HEMTs show typical $1/f$ low-frequency noise, as shown in Fig. 11(a). The noise magnitude was unchanged up to 1 Mrad(SiO₂) and increases by almost one order of magnitude after 100 Mrad(SiO₂), indicating activation of new border traps. Fig. 11(b) plots the low-frequency noise magnitude at 10 Hz as a function of V_{gt} in the HEMTs irradiated in “CUT-OFF”-bias condition. The devices show significant increases of the low-frequency noise levels at 100 Mrad(SiO₂), corresponding to the V_{th} increase and g_m decrease visible in Fig. 11. In both pristine and irradiated devices, the slope $|\beta|$ of $S_{id-V_{gt}}$ is ~ 2.1 indicating an approximately uniform spatial and energetic distribution of traps [27]-[29] before and during the irradiation. During room temperature annealing, the value of $|\beta|$ is 2.4, indicating a slightly non-uniform redistribution of the traps.

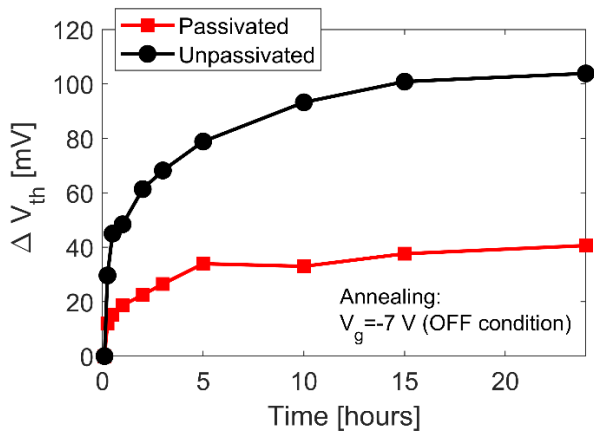


Fig. 10. Change in threshold voltage ΔV_{th} vs. time in passivated and unpassivated GaN-based HEMTs. The ΔV_{th} is measured during room temperature annealing of devices that were irradiated to 100 Mrad(SiO₂). The annealing is performed at $V_g = -7$ V, i.e., in the OFF-bias condition.

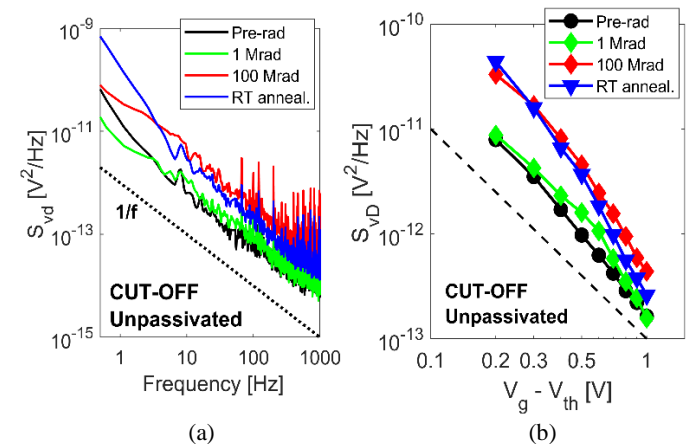


Fig. 11. (a) Low-frequency noise magnitudes for unpassivated GaN HEMTs irradiated in the “CUT-OFF”-bias condition. The noise was measured at $V_{ds} = 0.1$ V and $V_{gt} = 0.5$ V at room temperature. (b) $1/f$ noise magnitudes at $f = 10$ Hz vs. $V_{gs} - V_{th}$ at $V_{ds} = 0.1$ V for the “CUT-OFF” irradiated HEMT.

B. TID mechanisms

These results suggest two main TID-related mechanisms:

- *1st mechanism*. This is characterized by negative V_{th} shifts, g_m increases, and unchanged noise. In unpassivated devices, this response is visible under all bias conditions, with enhancement at high gate biases. It is likely that this mechanism results from the TID-assisted passivation of acceptor-like defects via hole capture [16], [32].

- *2nd mechanism*. This is characterized by positive V_{th} shifts, g_m degradation, and increase of the low-frequency noise magnitude. It is visible only during the irradiation at high gate biases, i.e., “CUT-OFF” and “OFF” at doses >10 Mrad(SiO₂). It is more likely that this mechanism is related to activation of acceptor-like defects via dehydrogenation of defects, as often observed in proton-irradiated GaN-based HEMTs at higher fluences [15], [16], [18], [29].

C. Leakage current

Fig. 12 plots the off-state leakage current I_{off} flowing through the drain terminal when $V_{gs} = -7$ V and $V_{ds} = 5$ V in unpassivated HEMTs. In general, the value of I_{off} increases by about one order of magnitude after devices are irradiated to 100 Mrad(SiO₂), with negligible contributions of electrical stress (dotted curves). Only GaN-based HEMTs in the “CUT-OFF”-bias condition (green curves) exhibit these large I_{off} increases of about two orders of magnitude. This high I_{off} degradation in “CUT-OFF” biased HEMTs is induced by electrical stress, which is enhanced when the gate and drain are simultaneously biased at opposite voltages. The high electric field induced by high gate-to-drain voltage may lead to percolation-based transport through defect and/or impurity centers in the AlGaN layer [20], [29], [35]-[37]. Particularly at higher voltages, these stress conditions may also lead to impact ionization of carriers, leading to positive charge trapping in the passivation layer of these devices [37], [38].

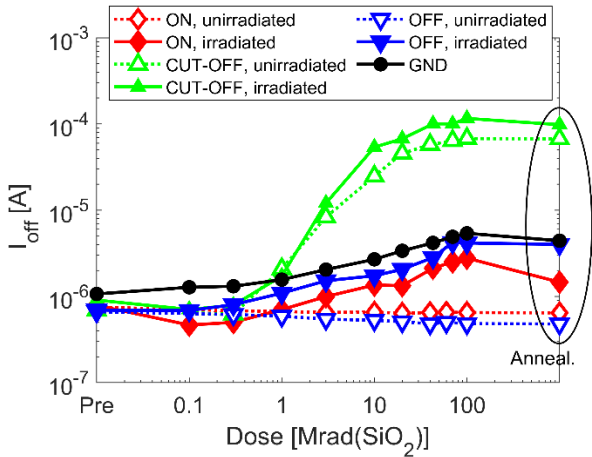


Fig. 12. Increase of the drain leakage current I_{off} at $V_{ds} = 5$ V as a function of cumulative dose for GaN HEMTs irradiated and annealed in different bias conditions.

V. DISCUSSION

Fig. 13 shows the ΔV_{th} and gate leakage I_g of passivated and unpassivated HEMTs irradiated and annealed under different bias conditions. The “CUT-OFF” and “OFF”- biased HEMTs

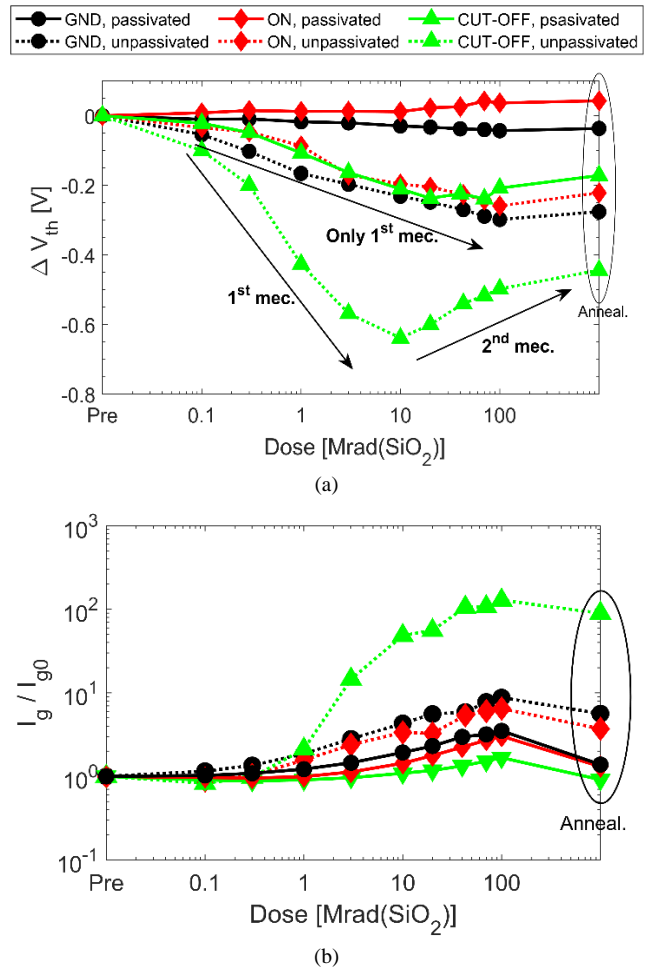


Fig. 13. Degradation of (a) threshold voltage ΔV_{th} and (b) gate leakage current I_g/I_{g0} for passivated and unpassivated GaN-based HEMTs. Solid lines refer to passivated devices, while dotted lines refer to unpassivated devices. Irradiations are performed up to 100 Mrad(SiO₂) and then devices were annealed at room temperature for 27 h under similar bias conditions to those applied during irradiation.

have similar TID responses; only “CUT-OFF”-biased devices are shown for clarity. The trends of curves in Fig. 13(a) among passivated and unpassivated devices are generally similar, except for passivated “ON”-biased devices, for which the degradation is dominated by electrical stress. TID-induced effects are enhanced when bias is applied to the gate, i.e., at $V_g = -7$ V, corresponding to the OFF condition. In “CUT-OFF” passivated and unpassivated devices, TID effects are caused by the two mechanisms described in section IV. The 1st mechanism occurs at doses <10 Mrad(SiO₂) with negative V_{th} shifts, while the 2nd mechanism dominates at doses > 10 Mrad(SiO₂) with positive V_{th} shifts. “GND” and “ON” biased devices exhibit only the 1st mechanism, inducing negative V_{th} shifts.

Observed shifts in Fig. 13(a) are smaller for passivated devices than unpassivated devices. After 100 Mrad(SiO₂) in the “CUT-OFF” bias condition, V_{th} values for the passivated HEMTs shifts by -0.34 V vs. -0.68 V for unpassivated devices. The higher TID sensitivity of unpassivated HEMTs compared to passivated devices highlights the key role of contaminant absorption (e.g., oxygen, moisture) through the surface layers [21], [23]. SiN_x passivation inhibits moisture absorption, limiting the formation of acceptor-like defects [21]. Hence, the

composition and thickness of passivation layers is an important factor in determining the radiation tolerance and long-term reliability of GaN-based HEMTs.

Fig. 13(b) shows the gate current I_g normalized by its pre-irradiation value of I_{g0} for GaN-based HEMTs irradiated under different bias conditions. In general, the highest gate-to-drain leakage currents are visible in unpassivated devices. After 100 Mrad(SiO_2), the value of I_g/I_{g0} of unpassivated HEMTs increases by roughly one order of magnitude for all cases except CUT-OFF devices. These show increases of two orders of magnitude, consistent with the stress-induced increase visible in I_{off} in Fig. 12. In passivated devices, the increase of the gate leakage is lower than one order of magnitude, regardless of bias applied during irradiation. Since the leakage depends only weakly on gate bias, the leakage in the passivated devices is dominated most likely by charge trapping in the SiN layer [35], [36], while unpassivated devices are most likely dominated by surface trap buildup at the top of the AlGaIn [37], [38]. Both the traps in SiN and the surface traps are most likely charged positively after stress, based on the behavior of the device of Fig. 12, and consistent with the electric fields. The comparative responses between the two device types in Fig. 13(b) suggest that the surface trap density in the unpassivated devices exceeds the SiN charged trap density [23].

VI. CONCLUSIONS

AlGaIn/GaN HEMTs irradiated at ultra-high doses show significant degradation due to TID and electrical stress, with magnitudes depending on irradiation bias. In general, ultra-high doses induces negative V_{th} shifts with magnitudes that are higher than the ones retrieved at lower doses of previous X-rays and gamma studies. The HEMTs irradiated with negative gate bias (OFF-state) exhibit the most negative threshold voltage shifts. At doses <10 Mrad(SiO_2), TID effects are related to the passivation of pre-existing acceptor-like defects via hole capture, which induces negative threshold voltage shifts and improvement of transconductance. At doses >10 Mrad(SiO_2), dehydrogenation of defect and impurity complexes leads to the creation of acceptor-like defects. These degrade the transconductance, shift the threshold voltage positively, and increase low-frequency noise. Slight performance recovery is visible after 27 h of room temperature annealing, most likely due to the formation of a significant density of stable defects.

Irradiation results on passivated and unpassivated HEMTs show that passivation layers may strongly affect oxygen and moisture absorption. The enhanced degradation of unpassivated devices in this study reinforces the key role that oxygen impurities and hydrogen play in the radiation response and long-term reliability of GaN-based HEMTs.

Considering potential system applications, AlGaIn/GaN HEMTs have much greater tolerance to ultra-high doses than Si-based CMOS technologies [1], [2], [9], [12], [15]. In the worst-case condition, AlGaIn HEMTs show $<10\%$ ΔI_{on} variation after 100 Mrad(SiO_2), which is less than $\sim 38\%$ of 31 nm MOSFETs and $\sim 20\%$ of gate-all-around Si nano-wire FETs, both tested at ultra-high doses [1], [12]. Hence, the long-term reliability of the AlGaIn/GaN HEMTs is likely to be a more limiting factor than their radiation response [15], [18], [20].

REFERENCES

- [1] S. Bonaldo, *et al.*, "Ionizing-radiation response and low-frequency noise of 31-nm MOSFETs at ultra-high doses," *IEEE Trans. Nucl. Sci.*, vol. 67, no. 7, pp. 1332-1341, July 2020.
- [2] F. Faccio, *et al.*, "Radiation-induced short channel (RISCE) and narrow channel (RINCE) effects in 65 and 133 nm MOSFETs," *IEEE Trans. Nucl. Sci.*, vol. 62, no. 6, pp. 32663-3270, Dec. 2015.
- [3] S. Bonaldo, *et al.*, "Charge buildup and spatial distribution of interface traps in 65-nm pMOSFETs irradiated to ultrahigh doses," *IEEE Trans. Nucl. Sci.*, vol. 66, no. 7, pp. 1574-1583, July 2019.
- [4] F. Faccio, *et al.*, "Influence of LDD spacers and H^+ transport on the total-ionizing-dose response of 65-nm MOSFETs irradiated to ultrahigh doses," *IEEE Trans. Nucl. Sci.*, vol. 65, no. 1, pp. 164-174, Jan. 2018.
- [5] S. Gerardin, *et al.*, "Impact of 27-GeV proton irradiation on 0.13- μm CMOS devices," *IEEE Trans. Nucl. Sci.*, vol. 53, no. 4, pp. 1917-1922, Aug. 2006.
- [6] C.-M. Zhang, *et al.*, "Characterization of Gigard total ionizing dose and annealing effects on 31-nm bulk MOSFETs," *IEEE Trans. Nucl. Sci.*, vol. 64, no. 10, pp. 2939-2947, Oct. 2017.
- [7] S. Bonaldo, *et al.*, "Influence of halo implantations on the total ionizing dose response of 31-nm pMOSFETs irradiated to ultrahigh doses," *IEEE Trans. Nucl. Sci.*, vol. 66, no. 1, pp. 82-90, Jan. 2019.
- [8] S. Mattiazzo *et al.*, "Total ionizing dose effects on a 28 nm hi-K metal-gate CMOS technology up to 1 Grad," *J. Instrum.*, vol. 12, no. 2, Art. no. C02003, Feb. 2017.
- [9] T. Ma, *et al.*, "TID degradation mechanisms in 16 nm bulk FinFETs irradiated to ultra-high doses," *IEEE Trans. Nucl. Sci.*, vol. 68, no. 8, pp. 1571-1578, Aug. 2021.
- [10] T. Ma, *et al.*, "Influence of fin- and finger-number on TID degradation of 16 nm bulk FinFETs irradiated to ultra-high doses," *IEEE Trans. Nucl. Sci.*, vol. 69, no. 3, pp. 337-343, Mar. 2022.
- [11] S. Bonaldo, *et al.*, "DC response, low-frequency noise, and TID-induced mechanisms in 16-nm FinFETs for high-energy physics experiments," *Nucl. Instrum. Methods. Phys. Res. B*, vol. 1036, Art. no. 166730, June 2022.
- [12] S. Bonaldo, *et al.*, "TID effects in highly scaled gate-all-around Si nanowire CMOS transistors irradiated to ultra-high doses," *IEEE Trans. Nucl. Sci.*, vol. 69, no. 7, pp. 1444-1452, July 2022.
- [13] E. C. H. Kyle, S. W. Kaun, P. G. Burke, F. Wu, Y.-R. Wu, and J. S. Speck, "High-electron-mobility GaN grown on free-standing GaN templates by ammonia-based molecular beam epitaxy," *J. Appl. Phys.*, vol. 115, no. 19, Art. no. 193702, May 2014.
- [14] A. Ionascut-Nedelscu, C. Carlone, A. Houdayer, H. J. von Bardeleben, and J. L. Cantin, "Radiation hardness of gallium nitride," *IEEE Trans. Nucl. Sci.*, vol. 49, no. 6, pp. 3036-3038, Dec. 2002.
- [15] D. M. Fleetwood, E. X. Zhang, R. D. Schrimpf and S. T. Pantelides, "Radiation effects in AlGaIn/GaN HEMTs," *IEEE Trans. Nucl. Sci.*, vol. 69, no. 5, pp. 1105-1119, May 2022.
- [16] R. Jiang, *et al.*, "Worst-case bias for proton and 10-keV X-ray irradiation of AlGaIn/GaN HEMTs," *IEEE Trans. Nucl. Sci.*, vol. 64, no. 1, pp. 218-228, Jan. 2017.
- [17] R. Jiang, *et al.*, "Dose-rate dependence of the total-ionizing-dose response of GaN-based HEMTs," *IEEE Trans. Nucl. Sci.*, vol. 66, no. 1, pp. 170-176, Jan. 2019.
- [18] J. Chen, *et al.*, "Effects of applied bias and high field stress on the radiation response of GaN/AlGaIn HEMTs," *IEEE Trans. Nucl. Sci.*, vol. 62, no. 6, pp. 2726-2733, Dec. 2015.
- [19] T. Roy, *et al.*, "Electrical-stress-induced degradation in AlGaIn/GaN high electron mobility transistors grown under gallium-rich, nitrogen-rich, and ammonia-rich conditions," *Appl. Phys. Lett.*, vol. 96, no. 13, Art. no. 136803, Mar. 2010.
- [20] R. Jiang, *et al.*, "Multiple defects cause degradation after high field stress in AlGaIn/GaN HEMTs," *IEEE Trans. Dev. Mater. Reliab.*, vol. 18, no. 3, pp. 364-376, Sept. 2018.
- [21] R. Jiang, *et al.*, "Degradation and annealing effects caused by oxygen in AlGaIn/GaN high electron mobility transistors," *Appl. Phys. Lett.*, vol. 109, no. 2, Art. no. 026811, Jul. 2016.
- [22] S. Kaun, M. H. Wong, U. K. Mishra, and J. S. Speck, "Molecular beam epitaxy for high-performance Ga-face GaN electron devices," *Semicond. Sci. Technol.*, vol. 31, no. 7, Art. no. 074001, June 2013.
- [23] R. Jiang, *et al.*, "Total ionizing dose effects in passivated and unpassivated AlGaIn/GaN HEMTs," Proc. RADECS 2016, Bremen, Germany, Sept. 19-26, 2016, paper A-3.

- [24] A. Dasgupta, D. M. Fleetwood, R. A. Reed, R. A. Weller, and M. H. Mendenhall, "Effects of metal gates and back-end-of-line materials on x-ray dose in HfO₂ gate oxide," *IEEE Trans. Nucl. Sci.*, vol. 58, no. 6, pp. 3139-3144, Dec. 2011.
- [25] A. Dasgupta, D. M. Fleetwood, R. A. Reed, R. A. Weller, M. H. Mendenhall, and B. D. Sierawski, "Dose enhancement and reduction in SiO₂ and high- κ MOS insulators," *IEEE Trans. Nucl. Sci.*, vol. 57, no. 6, pp. 3463-3469, Dec. 2010.
- [26] S. K. Dixit, X. J. Zhou, R. D. Schrimpf, D. M. Fleetwood, S. T. Pantelides, R. Choi, G. Bersuker, and L. C. Feldman, "Radiation induced charge trapping in ultrathin HfO₂-based MOSFETs," *IEEE Trans. Nucl. Sci.*, vol. 54, no. 6, pp. 1883-1890, Dec. 2007.
- [27] M. R. Shaneyfelt, D. M. Fleetwood, J. R. Schwank, and K. L. Hughes, "Charge yield for 10-keV x-ray and cobalt-60 irradiation of MOS devices," *IEEE Trans. Nucl. Sci.*, vol. 38, no. 6, pp. 1187-1194, Dec. 1991.
- [28] P. F. Wang, *et al.*, "Worst-case bias for high voltage, elevated-temperature stress of AlGaIn/GaN HEMTs," *IEEE Trans. Dev. Mater. Reliab.*, vol. 20, no. 2, pp. 420-431, Jun. 2020.
- [29] J. Chen, *et al.*, "Proton-induced dehydrogenation of defects in AlGaIn/GaN HEMTs," *IEEE Trans. Nucl. Sci.*, vol. 60, no. 6, pp. 4080-4086, Dec. 2013.
- [30] D. M. Fleetwood, "1/f noise and defects in microelectronic materials and devices," *IEEE Trans. Nucl. Sci.*, vol. 62, no. 4, pp. 1462-1486, Aug. 2015.
- [31] D. M. Fleetwood, "Total-ionizing-dose effects, border traps, and 1/f noise in emerging MOS technologies," *IEEE Trans. Nucl. Sci.*, vol. 67, no. 7, pp. 1216-1270, Jul. 2020.
- [32] P. Wang, *et al.*, "1/f noise in as-processed and proton-irradiated GaN/AlGaIn HEMTs due to carrier-number fluctuations," *IEEE Trans. Nucl. Sci.*, vol. 64, no. 1, pp. 181-189, Jan. 2017.
- [33] G. Ghibaudo, O. Roux, C. Nguyen-Duc, F. Balestra, and J. Brini, "Improved analysis of low frequency noise in field-effect MOS transistors," *Phys. Stat. Sol.(a)*, vol. 124, no. 2, pp. 571-581, Apr. 1991.
- [34] J. H. Scofield, N. Borland, and D. M. Fleetwood, "Reconciliation of different gate-voltage dependencies of 1/f noise in nMOS and pMOS transistors," *IEEE Trans. Electron Devices*, vol. 41, no. 11, pp. 1946-1952, Dec. 1994.
- [35] J. W. Chung, J. C. Roberts, E. L. Piner, and T. Palacios, "Effect of gate leakage in the subthreshold characteristics of AlGaIn/GaN HEMTs," *IEEE Electron Device Lett.*, vol. 32, no. 11, pp. 1196-1198, Nov. 2008.
- [36] N. Xu, *et al.*, "Gate leakage mechanisms in normally off p-GaN/AlGaIn/GaN high electron mobility transistors," *Appl. Phys. Lett.*, vol. 113, no. 15, Art. no. 152104, Oct. 2018.
- [37] H. Yu, *et al.*, "Leakage mechanism in ion implantation isolated AlGaIn/GaN heterostructures," *J. Appl. Phys.*, vol. 134, no. 3, Art. no. 038701, Jan. 2022.
- [38] D. K. Sahoo, R. K. Lal, H. Kim, V. Tilak, and L. F. Eastman, "High-field effects in silicon nitride passivated GaN MODFETs," *IEEE Trans. Electron Devices*, vol. 50, no. 5, pp. 1163-1170, May 2003.